

V-Reactor Dynamics: Dual Chaotic System and Rewriting the Antiviral Response History

Yong-Shou Chen

China Institute of Atomic Energy, Beijing 102413, China

The COVID-19 pandemic revealed a key vulnerability: our failure to anticipate novel viral threats. Moving beyond descriptive virology, we introduce V-Reactor Dynamics (V-Dynamics), a physics-based framework modeling host-virus interaction as a synchronized dual chaotic system. This paradigm predicts viral evolution, immune response, transmission, and virulence through equations governed by the parameter reactivity (ρ). It quantifies infection phases, peak ($\rho > 0$), plateau ($\rho \approx 0$), clearance ($\rho < 0$), transmission, and modality via ρ/ℓ (Reactivity/Generation time). Retrospectively, it correctly predicted SARS-CoV-2's higher transmissibility versus SARS-CoV's lethality and forecasted Omicron waves, exposing the lockdown-socioeconomic cost trade-off. We introduce measurable constants, viral replication, immune evasion, and drug absorption cross sections, derived from in vitro virion interactions. These quantum mechanical analogues relate to ρ and ℓ , enabling pre-outbreak predictive surveillance. V-Dynamics reveals a duality: microscopic chaos in viral production and macroscopic chaos in population transmission, linked by a scaling law. The sign of ρ , tied to the Lyapunov Exponent, dictates pandemic trajectory ($\rho > 0$ for outbreak, $\rho < 0$ for termination), offering a control mechanism. By unifying kinetics, cross-scale dynamics, and chaos theory, this framework provides a quantitative roadmap to preempt future pandemics.

Throughout history, the human immune system has been engaged in a relentless struggle against viral evolution, a challenge that remains fundamentally unresolved. Despite significant advances in medicine and genomics, the COVID-19 pandemic revealed critical vulnerabilities in our global defense strategies. SARS-CoV-2, a virus with substantial genetic similarity to earlier coronaviruses^[1] infected over 676 million people and claimed 6.88 million lives by March 2023^[2], dwarfing the scale of the 2003 SARS outbreak (8,096 cases, 774 deaths)^[3]. This stark discrepancy underscores a pivotal failure: genomic surveillance alone proved insufficient to predict the emergent high transmissibility and pathogenicity of COVID-19, exposing a grave gap in pandemic preparedness. The core lesson of the pandemic is the recurring inadequacy of our immune defense and public health systems against novel viral variants. This pattern highlights the limitation of a reactive, sequence-dependent approach to virology. While recent initiatives like the WHO Pandemic Agreement emphasize the crucial sharing of pathogen genetic data^[4], they still operate within a paradigm that cannot fully anticipate or mitigate the threat of future variants. The persistent shortfall in pandemic prevention and response stems from a lack of an original scientific framework capable of a paradigm shift from descriptive

to predictive virology. To address this critical gap, we introduce V-Reactor dynamics (V-dynamics), a novel physics-based framework that reconceptualizes host-virus interactions as a dual chaotic system. By integrating principles from quantum mechanics, particle diffusion, nuclear physics, and chaos theory, V-dynamics moves beyond the constraints of genetic data alone. This innovative framework provides a comprehensive, predictive model, which integrates both theoretical and experimental approaches, to synchronize human immune defense with viral evolution. It is designed to accurately forecast viral behavior and pandemic potential, thereby enabling a new era of precision antiviral strategies characterized by early warning systems and cost-effective interventions.

Concepts of V-reactor dynamics

The Cononavirus(V)-reactor dynamics is introduced from physics viewpoint to explain the SARS-CoV-2 infection in human lung and its pandemic. Here its key concepts are put forward.

Virion replication reaction. A virion replication reaction is a viral reaction where the target H-particle (host cell) is bombarded by a virion, and subsequently undergoes a transformation into a destroyed H-particle, with a release of new virions. The released virions can then strike other H-particles, creating a chain reaction that can be controlled in a disease lung core or uncontrolled in resulting death.

Self-sustaining virion chain reaction. A self-sustaining virion chain reaction is a viral replication process where virions released from the replication of one H-particle collide with and cause other H-particles to destroy, releasing more virions in a continuous, self-amplifying cascade. This process becomes self-sustaining when, on average, each replication event produces enough virions to trigger at least one more replication event, preventing the reaction from dying out. In a V-reactor, the virion chain reaction is controlled often through the immune responses to the virus, where the virions are absorbed (neutralized) by the A-particles (antibodies), leading to a transient balance between production and destruction of virions.

V-reactor hypothesis. Our hypothesis posits that the diseased human lung, a complex biological system infected by viruses, can be modeled through physics-based perspective as a virion V-reactor similar to a neutron reactor. The self-sustaining virion chain reaction is the central concept of V-reactor. This may be examined by the idea statement: "a V-reactor is an assembly of human lung material which is capable of self-sustaining and controlling a virion chain reaction with a H-particle fuel." The self-sustaining virion chain reaction has been observed, for example, in the laboratory experiment, performed for the study of the replication reaction by utilizing inoculated human lung tissue explants with SARS-CoV-

2 or SARS-CoV, and the results show that the number of virions grows a hundredfold from 2 to 48 hours for SARS-CoV-2^[5].

Core equations in V-reactor dynamics

The fundamental equations for the V-reactor dynamics have been derived starting from the diffusion equation describing that virions move randomly through the reactor core, undergoing processes such as scattering, absorption, and leakage (see Methods.)

Viral kinetic equation. The viral kinetic equation is derived from the virion diffusion equation under the assumptions that lead to the point reactor model (see Methods),

$$\frac{dn_V(t)}{dt} = \frac{\rho}{\ell} n_V(t), \quad (1)$$

describing how the virion density $n_V(t)$ changes over time as virions diffuse through the reactor core, lost by absorption and leakage, and create new virions through replication. Where the reactivity ρ and the generation time ℓ can be expressed as:

$$\rho = \frac{k_{eff} - 1}{k_{eff}}, \ell = \frac{\ell_0}{k_{eff}}. \quad (2)$$

Where k_{eff} is the effective multiplication constant, denoting the ratio of the average number of virions produced to the average number of virions lost by absorption and leakage. Where ℓ_0 is the virion effective lifetime, denoting the mean time for one virion to be lost by absorption and leakage. For integration of kinetic equation (1), the limits are $n_V(t) = n_V^0$ at $t = 0$, $\rho = 0$ at $t < 0$, $\rho = \rho$ at $t = 0^+$ and $n_V(t) = n_V(t)$ at $t = t$. Generally, ρ is time-dependant and the solution to Eq. (1) can be written as:

$$n_V(t) = n_V^0 \exp\left(\frac{1}{\ell} \int_0^t \rho(t) dt\right). \quad (3)$$

In the present modeling, the basic mode of reactivity is $\rho(t) = \rho_0 - \gamma t$, where $\rho_0 \geq 0$ and $\gamma \geq 0$, and the corresponding solution can be expressed as:

$$n_V(t) = n_V^0 \exp\left(\frac{\rho_0}{\ell} t - \frac{\gamma}{2\ell} t^2\right). \quad (4)$$

Burnup equation of H-particles. The burnup equation describes decline in the concentration of H-particles, as fuel materials, due to viral replication, where cellular burnout severity determines clinical mortality. We assume that the H-particle undergoing replication or capture reactions will transform into a destructed H-particle, no longer considered as fuel. By neglecting the influence of consumption of H-particles in return on the virion flux, the burnup equation may be written as (see Methods):

$$\frac{dN_H(t)}{dt} = -\sigma_a \phi N_H(t), \quad (5)$$

Where N_H is the density of H-particles, σ_a the cross section for virion absorption, which is the sum of capture and replication cross sections, $\sigma_a = \sigma_c + \sigma_r$, and $\phi = v n_V$ denotes the virion flux in the disease lung core. The fuel burnup or consumption is defined as the percentage fraction, N_H/N_H^0 . The inclusion of the virion absorption cross section and the virus flux in the burnup equation highlights the complex interplay between viral load and host cell susceptibility.

Equation of viral spread. This theory seeks to bridge molecular scale (virion behavior) and macroscopic scale (epidemic spread). By integrating viral dynamics with chaos theory, we derived a viral transmission equation for the number of people testing positive to the virus, N_{pos} , which can be expressed as (see Methods):

$$N_{pos}(d) = \frac{N_0 N_\infty}{N_0 + N_\infty \exp(-\lambda d)}. \quad (6)$$

Where λ is so called the Lyapunov Exponent (LE) for the chaotic system, d (in days) represents the time from the start of the epidemic or the beginning of testing to isolate the virus, $N_0 = N_{pos}(t = 0)$ is the initial number of people from whom the infection started. As a chaotic system, the function $N_{pos}(t)$ is inherently constrained by certain conservation laws, leading to a finite saturation value $N_\infty = N_{pos}(t \rightarrow \infty)$. Eq.(6) provides an useful tool to analyze the viral spreading data by parameter fitting, and to simulate the progression and impacts of pandemic on public health, society, and the economy, thereby providing scientific data to optimize pandemic response strategies.

Virion interaction cross sections

This research approach bridges quantum mechanics and virology, pioneering a bold and unconventional direction. The framework treats virus particles and cells as quantum mechanical entities with well-defined cross sections. The V-dynamics theory introduces three fundamental cross sections that quantify viral interactions with their environment. Cross section for virion replication with host cells (σ_r) measures the probability of successful viral replication with a host cell and releasing new virions, reflecting viral and host adaptability (e.g., ACE2 binding efficiency for SARS-CoV-2). It can predict viral load dynamics and transmissibility. Cross section for virion absorption (neutralization) with antibodies (σ_a) quantifies the probability of antibody-mediated neutralization, determining immune escape potential (e.g., mutations in the spike protein reducing σ_a). It is used for vaccine efficacy assessment and variant risk forecasting. Cross section for virion absorption with drugs (σ_d^D) defines the likelihood of a drug molecule successfully binding and inhibiting a virion, indicating drug resistance risk (e.g., influenza vs. SARS-CoV-2 susceptibility to antiviral). It guides rational drug design by optimizing σ_a^D for broad-spectrum efficacy. Based on quantum mechanics we provided computational method for cross section calculation. Importantly, the V-dynamics proposes measuring the cross sections of virus-host interactions through in vitro experiments, enabling precise prediction of viral infection efficiency.

Reactivity and generation time

The reactivity and generation time are the two fundamental viral dynamic parameters. The reactivity ρ is equal to the ratio of the net growth in number of virions to the number of virions produced, and the generation time ℓ is inversely proportional to the virion production per second, and they can be expressed as:

$$\rho = 1 - \frac{\Sigma_a + DB^2}{\nu \Sigma_r}, \ell = \frac{1}{\nu \Sigma_r}. \quad (7)$$

Where ν is the average number of virions produced per replication, ν the thermal velocity of virions, $\Sigma_r = \sigma_r N_H$ is the macroscopic cross sections for replication, where N_H is host cells density, and $\Sigma_a = \sigma_a N_A$ is the macroscopic cross sections for absorption (neutralization), where N_A is antibodies density. DB^2 represents the leakage loss term. The reactivity rate ρ/ℓ , representing the exponential growth rate of viral load, varying with reactivity and referred to as "reactivity" in this study unless otherwise specified. It is expressed as

$$\rho/\ell = \nu(\nu \Sigma_r - \Sigma_a - DB^2), \quad (8)$$

describing quantitatively the dynamic balance between viral replication and immune defense during infection. Viral pathogenicity is characterized by the viral replication cross section $\nu \sigma_r$, while viral immune escape capability is quantified by the antibody absorption cross section σ_a . In a case of medicine intervention, the drug efficacy is measured by the drug absorption cross section σ_a^D ,

which contributes to ρ/ℓ via an additional reduction term $-v\Sigma_a^D$ in Eq.(8), where $\Sigma_a^D = \sigma_a^D N_D$, and N_D denotes drug particle density.

Dual chaotic systems and rate scaling law

The cornerstone of V-dynamics lies in the discovery of dual chaotic systems, microscopic viral production chaos and macroscopic population transmission chaos, linked by a rate scaling law. Viral pandemics emerge from the dynamic coupling of these two chaotic systems. The dynamical control parameter of chaotic systems is termed the Lyapunov Exponent (LE), which quantifies the divergence between two initially infinitesimally close trajectories (events) in phase space over time t . V-dynamics introduces a quantitative paradigm to measure the unpredictability of viral evolution and transmission, proposing Lyapunov Exponent (LE) control as a mechanism for pandemic intervention. The kinetic equation (1) indicates that the viral load, $n_V(t)$, grows exponentially at a rate characterized by the initial reactivity, ρ_0/ℓ . As the peak viral load dominates the total viral production, its exponential growth, $n_V(t) = n_0 \exp((\rho_0/\ell)t)$, can be interpreted as a chaotic process. In this framework, the (LE) of this viral production chaos is defined by the initial growth rate, $\lambda_V = \rho_0/\ell$. The chaotic divergence, $d(t)$, is thus analogous to the viral load itself. This leads to a logistic growth-like model for $n_V(t)$: $n_V(t) = (n_0 n_\infty) / (n_0 + n_\infty \exp(-\lambda_V t))$. Where $n_0 = n_V(t=0)$, $n_\infty = n_V(t \rightarrow \infty)$, and λ_V is the Lyapunov exponent governing the chaotic growth. The transmission dynamics within a population, represented by the number of positive cases $N_{pos}(t)$ in Eq.(6), evolve on a slower timescale than the intra-host viral load. We postulate a power-law relationship between the fast-varying viral load and the slower-varying case count: $N_{pos}(t) = n_V(t)^\chi = N_0 \exp(\chi(\rho/\ell)t)$, where χ is a dimensionless scaling exponent. This relationship implies that the growth rate of the population-level outbreak is scaled by the exponent χ . Consequently, the Lyapunov exponent λ for the population transmission chaos is given by the scaling law: $\lambda = \chi \lambda_V$. The value of the scaling exponent χ , which couples the intra-host and population-level dynamics, can be determined experimentally. Analysis of typical SARS-CoV-2 viral load and transmission data suggests χ values of $\sim 10^{-2}$ order. The viral load grows exponentially with a coefficient of ρ_0/ℓ , which is empirically about $0.15h^{-1}$ for SARS-CoV-2. In the absence of immune or other effective interventions, the chaotic system will eventually reach a state of extremely high viral load saturation, leading to patient death. For example, a sputum sample collected on day 8 post-onset from a patient who died had a very high viral load (1.34×10^{11} copies per ml), and, however, the peak viral loads of SARS-CoV-2 in all other clinical samples collected on day 3 post-onset were $\sim 1 \times 10^6$ copies per ml^[7]. In most cases, viral loads peak around 3 days after symptom onset, driven by a sharp decline in reactivity from positive to negative as the immune response activates. These patients are expected to fully recover, progressing through subsequent plateau and clearance phases of viral load, corresponding to near-zero and negative values of ρ , respectively. Critically, the key window for preventing progression to a dangerous state is the first few days after disease onset, before the system enters uncontrolled exponential growth. The reactivity, as a measurable physical quantity, offers actionable metrics not only for clinical intervention but also transmission control. Optimized antiviral interventions can drive the LE of virus production chaos toward negative values, subsequently inducing synchronized reversal in population transmission chaos. The sign reversal of both LEs marks the end of viral pandemic.

Viral dynamics of SARS-CoV-2

Based on the viral kinetic equation, we provide a quantitative de-

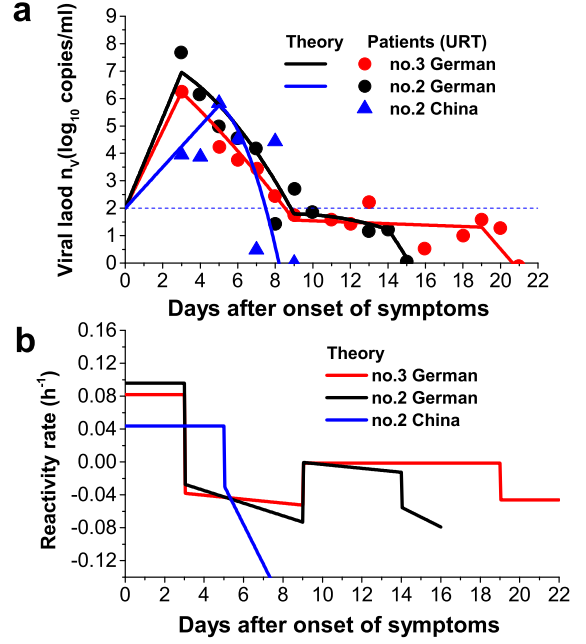


Figure 1: **a** Theoretical viral loads of SARS-CoV-2, $n_V(t)$, (solid lines) in a comparison with the URT viral load data in patients no.2 in China^[7], no.2 and no.3 in German, and the blue dash line is the detection limit^[6]. **b** The reactivity rate ρ/ℓ (in unites of hour⁻¹) used to generate the viral loads in **a**.

scription of the viral dynamics of SARS-CoV-2 by examining the interactions of virion with H-particles (viral replication) and virion with A-particles (immune responses). We analyzed the data for the patents no.2 and no.3 in German^[6], having the 14 days and 21 days infection periods, respectively, as well as the data for the patient no.2 in China^[7], having the infection period of 9 days.

Viral load dynamic phases. The viral load refers to the amount of viruses present in an infected individual's body, and is determined by the reactivity ρ/ℓ , the pivotal dynamic parameter governing the process of infection. In our modeling, the reactivity has a step-wise pattern, and each step contains a basic mode, $\rho(t) = \rho_0 - \gamma t$, and within the each step the viral road $n_V(t)$ is calculated by using the viral load Eq.(4). We will show that a fantastic discovery will be the distinct dynamic phases of viral load of SARS-CuV-2, and the phase transition, originated from the dramatic stepwise shifts of reactivity. By using the reactivity of multi-step form, the viral load time curves of SARS-CuV-2 for the three patients are calculated and shown in Figure 1 panel a in a comparison with experimental data from the URT. It is demonstrated that the calculated viral load time curves are consistent with the data within the data uncertainties. In particular, the overall trends of the viral dynamics have been well reproduced by the theory, demonstrating clearly the peak, plateau, and clearance phases in viral loads. Other mathematical models, such as the study^[8], reported similar viral load stages.

Origin of viral load phase transition. The viral dynamic phase transition is driven by the reactivity switching. The symbolic inversion of reactivity (e.g., viral replication dominance \rightleftharpoons neutralization dominance) marks a shift in the dynamic phase. The viral load time curves shown in Figure 1 panel a, are generated from the corresponding reactivities shown in Figure 1 panel b. It is seen that the peak and clearance phases are originated from a symbolic

inversion of reactivity ($\rho > 0 \rightarrow \rho < 0$), representing a reversal of net growth. The plateau phase is a quasi-equilibrium dynamic state with reactivity ($\rho \approx 0$), where the replication and neutralization rates nearly cancel out, representing the adaptive immune response. The viral load dynamics in SARS-CoV-2 infected individuals exhibit patient-specific characteristics, determined by the temporal changes of reactivity. Typical cases progress through three distinct phases: peak phase (viral growth), plateau phase (equilibrium), and clearance phase (immune dominance), with reactivity transitioning from $\rho > 0 \rightarrow \rho \approx 0 \rightarrow \rho < 0$ over approximately 14-21 days. Mild cases manifest only the peak phase, showing rapid reactivity shift from $\rho > 0$ to $\rho < 0$ within about 7 days. Uninfected individuals maintain clearance phase throughout, with initial reactivity $\rho_0 < 0$, indicating absolute immune superiority. Long-term COVID-19 cases maintain a long plateau phase keeping reactivity $\rho \approx 0$ over few months or longer. Real-time monitoring of reactivity enables precise timing for clinical interventions, with particular emphasis on therapeutic strategies during the critical peak phase. The dramatic stepwise changes in reactivity, shown in Figure 1 panel b, are triggered by immune responses. This mechanism is explained by Eq. (8), which states that the reactivity ρ can abruptly decrease to a negative value. This occurs when the macroscopic cross section for virion absorption, $\Sigma_a = \sigma_a N_A$, becomes sufficiently large due to a rapid increase in A-particle density N_A , a measure of immune defense. Conversely, the reactivity will shift from negative to positive values following a rapid decrease in N_A . Similarly, antiviral drugs can induce analogous reactivity changes. Drug intervention, represented by a prompt increase in drug particle density N_D , introduces an additional term $-\nu\sigma_a^D N_D$ to ρ/ℓ in Eq. (8), thereby quickly reducing the reactivity.

V-dynamics predictive capacity and accuracy

V-dynamics is a novel scientific framework capable of predicting the transmission speed and pathogenicity of viruses, forecasting their negative impacts on public health, society, and the economy, and providing a scientific data foundation for developing effective pandemic control strategies. The scientific basis of V-dynamics predictive accuracy lies in the discovery of the dual chaotic system architecture of viral dynamics and the governing principle that the Lyapunov Exponents (LE) of this chaotic system are directly determined by the reactivity ρ/ℓ . V-dynamics proposes strategies for prediction both at the early stage of an outbreak and before an outbreak occurs.

Prediction at the early stage of outbreak. Prediction at the early stage of an outbreak involves using initial patient viral load data to theoretically calculate and extract the reactivity ρ/ℓ , thereby determining the population transmission rate and virus virulence data. We conducted a retrospective simulation of predictions made during the early stage of the SARS-CoV-2 outbreak. Using viral dynamics equations we computationally analyzed viral load test data from multiple patients infected with SARS-CoV-2 and SARS-CoV. The calculated viral load of SARS-CoV-2 is shown in Figure 2 panel a and compared with the data from four SARS-CoV-2 patients in Germany^[6]. In Figure 2 panel b, the calculated viral load of SARS-CoV is shown in comparison with the data from fourteen SARS-CoV patients in China^[9]. The viral load time curves in a and b are generated from Eq.(4) by using the reactivities shown in Figure 2 panels c and d, respectively. These calculated viral loads may be regarded as typical or average ones for the two viruses. Their different patterns, particularly the peak position, indicate a distinction of resulting lethality between two viruses. The reactivity for SARS-CoV-2 has a four-steps pattern, while the reactivity for SARS-CoV presents only a two-steps form, and, crucially, the initial reactivity ρ_0/ℓ is about three times larger

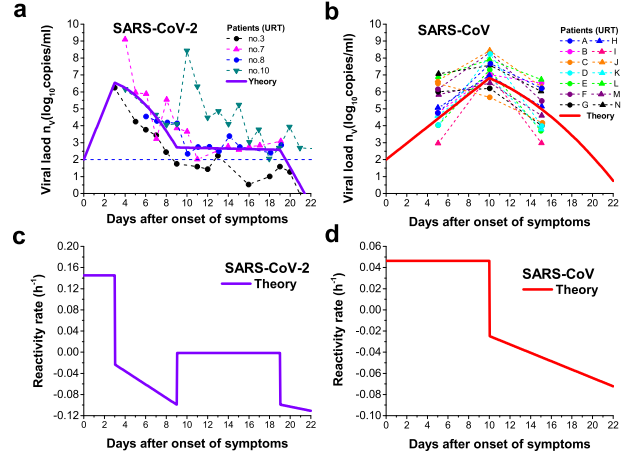


Figure 2: **a** The theoretical viral load of SARS-CoV-2 (violet solid curve) compared to the URT viral load data in patients no.3, no.7, no.8, and no.10 in Germany, and the blue dash line is the detection limit^[6]. **b** The theoretical viral load of SARS-CoV (red solid curve) compared to the URT viral load data in 14 patients in China^[9]. The viral load curves in **a** and **b** are generated by using the reactivity rates ρ/ℓ (in units of hour^{-1}) in **c** and **d**, respectively.

for SARS-CoV-2 than for SARS-CoV, indicating the triple transmission rate for the former.

-Viral transmission speed. To simulate viral transmission, the number of individuals testing positive for the virus, N_{pos} , was estimated for both SARS-CoV and SARS-CoV-2 using Eq.(6). The simulation was initialized with $N_0 = 10$ cases and propagated to a common final value of $N_\infty = 18,910.0$. The Lyapunov exponent (LE) values, characterizing the chaos in population transmission, were estimated as $\lambda = 0.05\rho_0/\ell$. This relationship adopts $\chi = 0.05$ in the scaling law, with the initial reactivity rates ρ_0/ℓ obtained from Figure 2 panels c and d. The results, presented in Figure 3 panel c, demonstrate that the time required for SARS-CoV-2 to reach N_∞ is only one-third of that required by SARS-CoV. This indicates that the transmission speed of SARS-CoV-2 is approximately three times greater than that of SARS-CoV.

-Host Cell Consumption (Burnup). The calculation of host cell (H-particle) consumption utilized the burnup equation (5), which requires the virion flux within the diseased lung core as an exposure input. Direct measurement of this flux is challenging due to the invasive nature of the required procedures. Consequently, we simulated it based on available upper respiratory tract (URT) viral load data. As URT viral loads represent accumulated quantities over time, we reasoned that the viral load in the lung core, while likely significantly lower, would follow a similar temporal trend. The simulated viral loads in the lung core for both viruses (Figure 3 a) were generated using the reactivity rates from Figure 2 c and d. Compared to the theoretical URT viral loads (Figure 2 a and b), the simulated lung core loads exhibit identical temporal trends but are scaled down by a factor of $1/500$. Using these virion fluxes as inputs and the theoretical absorption cross-section $\sigma_a = 2.775 \times 10^{-11} \text{ cm}^2$ (see Methods), the H-particle burnup was calculated (Figure 3 b). The results show that the majority of H-particle burnout occurs during peak virion flux exposure. SARS-CoV induces more pronounced host cell burnout, which correlates with its higher lethality and aligns with real-world data. Although H-particles are estimated to constitute only 1-10 percent of lung and airway cells^[10], significant burnout can lead to substantial tissue damage, inflammation, and organ dysfunction, thereby

contributing to observed mortality rates. Overall, the transmission

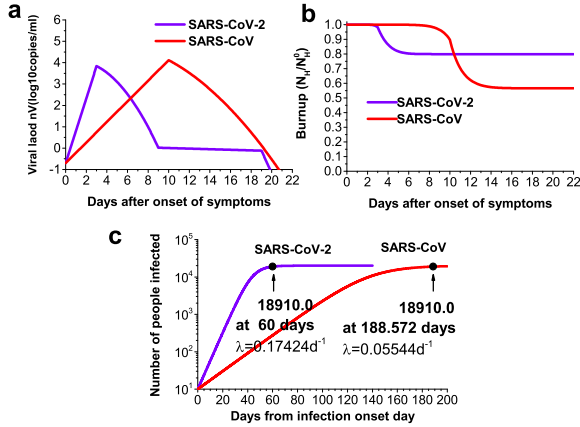


Figure 3: **a** The simulated viral loads in the lung core for SARS-CoV-2 (violet curve) and SARS-CoV (red curve), generated using the reactivity rates in Figure 2 panels c and d, respectively. **b** The burnup of H-particles, calculated from Eq. (5) using the corresponding viral loads in **a** as the virion flux inputs. **c** The number of people infected as a function of time, calculated by using Eq. (6) with the (LE) values, which are obtained as $\lambda = 0.05\rho_0/\ell$ using the scaling law with $\chi = 0.05$ and the initial reactivity rates in Figure 2 c and d.

and burnup calculations predict that a much higher viral transmission rate for SARS-CoV-2, but a higher mortality for SARS-CoV. Amazingly, in the two outbreaks, SARS-CoV-2 has proven to be more transmissible and to have a lower death rate than SARS-CoV [11, 12]. Although its mortality is lower, but due to its much higher transmission rate, SARS-CoV-2 has resulted in a much larger number of deaths globally.

-Real time clinical treatment. V-dynamics identifies three phases in typical SARS-CoV-2 infection: Peak phase ($\rho > 0$), viral proliferation dominates, Plateau phase ($\rho \approx 0$), a dynamic equilibrium is reached, and Clearance phase ($\rho < 0$), the immune system clears the infection. Real-time monitoring of the reactivity parameter not only provides scientific data for an early stage prediction but also enables precise timing for clinical intervention, especially during the critical peak phase. As ρ is a measurable quantity, it provides a data-driven basis for treatment. High-precision and rapid measurement of viral loads, necessary for early-stage outbreak prediction and individual clinic treatment, demands multidisciplinary collaboration and the application of AI technology. We propose an AI-driven Reactivity Tracking Tester (AI-RTT) to measure reactivity ρ/ℓ , whose development for clinical and experimental use presents a significant commercial opportunity in the medical device sector. This allows for personalized, real-time treatment adjustments and supports drug development by predicting patient response. This "tracing reactivity" strategy is applicable to other influenza viruses, and the development of this tester presents a significant commercial opportunity.

Pre-outbreak prediction. Prediction of potential outbreaks, including cross-species transmission prediction, is a novel concept for pre-outbreak viral forecasting. It starts from in vitro experimentally measured viral reaction cross section σ data to calculate reactivity ρ and generation time ℓ , which in turn are used to compute the viral transmission rate and virulence data. This represents a fundamental feature of the V-dynamics quantitative predictive science framework: an absolute predictive capability

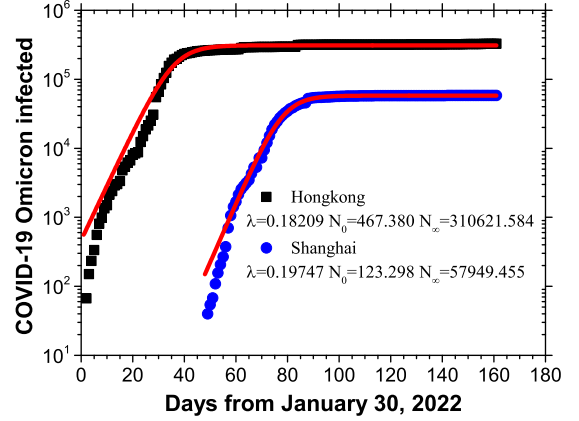


Figure 4: Comparison of computed number of people tested positive for COVID-19 variant Omicron virus with the experimental data for Hongkong (solid square) and Shanghai (solid circle). The fitted parameter values are marked in the graph.

based on laboratory measurements of virus-cell interaction constants. Here, the viral reaction cross section - a physical quantity describing microscopic bio-particle interactions, introduced based on quantum mechanics principles - along with the V-dynamics-derived relationships between reactivity, generation time, and the viral reaction cross section, form the key theoretical basis for pre-outbreak prediction. A new antiviral research strategy involving in vitro experimental measurement of virus interactions with cells, antibodies, and drug molecules, i.e., the viral reaction cross section, is a crucial step towards achieving a paradigm shift from descriptive to predictive virology. In vitro measurement of the viral reaction cross section is a new antiviral research direction we propose. Achieving high-precision and rapid experimental measurement of viral reaction cross sections requires multidisciplinary collaboration (integrating Physics, Biology, Virology, and Medicine) and the application of AI technology.

Forecasting prediction of impacts of local outbreaks. Once the initial reactivity rate is obtained from early-stage viral load data or pre-outbreak cross section data, we can perform an early prediction of LE for the population transmission chaotic system. This enables the forecasting of local outbreak impacts. We can simulate the progression and impact of local outbreaks by calculating the profile of the number of people testing positive to the virus, $N_{pos}(t)$, for different saturation infection levels N_∞ . This enables us to estimate public health burdens (e.g., the $N_{pos}(t)$ profile), social impacts (e.g., strict lockdowns and home isolation policies), and economic impacts (e.g., negative GDP growth). These forecasts provide a scientific basis for optimizing pandemic response strategies. Using the population transmission equation (6), we retrospectively simulated the spread of the SARS-CoV-2 Omicron variant and its negative impacts in Hong Kong and Shanghai. We fitted the transmission equation parameters to Omicron infection data from both cities [13]. As illustrated in Figure 4, the simulated infection curves for both cities exhibit a similar rising trajectory, indicating comparable transmission dynamics attributable to their shared viral origin. The results indicate that the saturation infection number N_∞ was approximately 310,000 for Hong Kong but only 58,000 for Shanghai. This discrepancy can be attributed to the strict lockdown and home isolation policies implemented in Shanghai, which significantly reduced the number of people exposed to the virus, thereby shrinking the virus transmission "phase space." It is worth reflecting that while Shanghai's pandemic response strategies drastically reduced infection num-

bers, they came at a high cost: the city experienced unprecedented negative economic growth in the first half of 2022.

In vitro measurement of virus-cell interactions

The V-reactor dynamics defines the constants of virus-cell interactions and proposes quantifying these functional parameters through in vitro experiments. This approach opens new interdisciplinary research avenues, generating quantitative data to precisely predict viral infectivity and transmission dynamics, a critical frontier in epidemic forecasting and antiviral innovation. Our experimental strategy aims to directly measure the functional parameters of virus-cell interactions, including the cross sections for viral replication with host cell particles, σ_r , for viral absorption (neutralization) by antibodies, σ_a , and for viral absorption by drug particles, σ_a^D . Quantifying these cross sections provides a scientific foundation not only for predicting virulence, transmission and outbreak potential but also for modeling the evolutionary trajectories of viral mutation and cross-species transmission. Achieving this goal requires the integration of biological and physical techniques. Specifically, we propose the development of high-precision, single-virus tracking methodologies, such as super-resolution microscopy coupled with micro-fluidics to directly observe and quantify viral replication events (e.g., particle binding, cell entry, and progeny virion release). Furthermore, advanced real-time data recording/analysis systems linked to the observation platform and specialized microchips must be engineered to enable rapid, high-throughput, and high-fidelity measurements. While the development of these precise in vitro tools presents a significant technical bottleneck, these challenges are surmountable through interdisciplinary collaboration and the integration of computational and AI technologies. Guided by the V-dynamics framework, this quantitative paradigm has the potential to revolutionize antiviral research by enabling a proactive synchronization of human defenses with the pace of viral evolution.

Conclusion

The V-dynamics introduces a fundamental paradigm shift from descriptive to predictive virology by examining virus from physics perspective. The scientific basis and validation of V-dynamics predictive accuracy lies in the discovery of the dual chaotic system architecture, the microscopic viral production chaos and the macroscopic population transmission chaos. The fundamental dynamic parameter reactivity ρ is identified to govern the entire infection process. The initial reactivity rate ρ_0/ℓ defines the LE of viral production chaos and determines, via a derived rate scaling law, the LE of population transmission chaos. Based on reactivity temporal dynamics, infection progression is divided into three phases, peak ($\rho > 0$), plateau ($\rho \approx 0$), and clearance ($\rho < 0$). Crucially, the sign of reactivity dictates pandemic fate, positive reactivity ($LE > 0$) drives outbreaks, while negative reactivity ($LE < 0$) ensures viral termination. V-dynamics enables prediction at two stages. Early-Outbreak Prediction utilizes early patient viral load data to calculate reactivity ρ/ℓ , immediately quantifying transmission and virulence. Retrospective analysis of SARS-CoV and SARS-CoV-2 data accurately predicted the latter's higher transmission and the former's greater fatality rate. Retrospective analysis for the Omicron waves in Hong Kong and Shanghai revealed a critical trade-off between strict public health measures and socioeconomic costs. This underscores the model's utility in forecasting virus risk and public health and economic impacts. More fundamentally, Pre-Outbreak Forecasting is a novel concept enabling prediction from first principles. It begins with in vitro measurements of viral reaction cross sections (σ) quantifying interactions between virions and host cells, antibodies, vaccines, or drug particles. These in vitro data are used to calculate reactivity ρ and gen-

eration time ℓ by using derived mathematical relationships among reactivity and cross sections, which in turn compute transmission rate and virulence. V-dynamics. This provides an absolute predictive capability based on virion-cell interaction data alone, enabling the prediction of LEs for both chaotic systems from experimental data. The integration of three key cross-sections, viral fitness (σ_r), immune evasion (σ_a), and drug resistance (σ_a^D), creates a unified biophysical framework for pre-emptively assessing emerging variants and accelerating the design of targeted countermeasures. Achieving the necessary high-precision, rapid measurement of viral reaction cross sections and viral loads demands multidisciplinary collaboration (integrating Physics, Biology, Virology, and Medicine) and the AI technology. V-dynamics reveals that viral evolution adheres to a singular principle: maximizing the LE of production chaos by optimizing fitness (σ_r) while minimizing immune susceptibility (σ_a), thereby ensuring dominance over host defenses. Similarly, cross-species transmission is theorized to favor jumps between hosts with comparable LE values and thus similar σ_r and σ_a profiles. By tracking these LE values, V-dynamics offers predictive insight into the directions of viral mutation and zoonotic transmission. The recurring inadequacy of reactive, sequence-dependent approaches against novel variants highlights an urgent need for a new paradigm. While global initiatives for genetic data sharing are crucial, they must be expanded to include the functional, quantitative data introduced by V-dynamics. In summary, V-dynamics redefines virology through physics-based predictability, marking an essential transition from observational to quantitative, predictive science. This paradigm shift, guided by a framework that spans theory and experimentation, promises to revolutionize antiviral research by synchronizing human defenses with viral evolution. It is designed to accurately predict virus transmission and virulence, forecast their impacts on public health, society and economics. As a cornerstone tool, V-dynamics promises a future of "early warning, low-cost" pandemic response, fundamentally transforming our preparedness for coronaviruses and beyond.

Acknowledgements The author thanks Evelyn Yan Jiang, AI engineer USA, for the valuable information on the SARS-CoV-2 pandemic. This research was supported by the Continuous Basic Scientific Research Project No. WDJC-2019-13, BJ20002501, and by the National Natural Science Foundation of China under Grant No. 11790325, No. 11975314.

Author contributions The author has proposed and designed this research and completed all aspects of this work as a contribution to win against the viral epidemics.

Author Information The author declares no competing financial interests. Readers are welcome to comment on the online version of the paper. Correspondence and requests for materials should be addressed to Y.-S. Chen (yshouchen@163.com).

Methods

Virion diffusion equation. Similar to the diffusion of neutrons in a nuclear reactor, the diffusion of virions in a V-reactor can be described by the diffusion equation. In the V-reactor core, a virion at a given position and time, with a specific kinetic energy and direction, will move to another position with different kinetic energy and direction at a later time. This phenomenon is known as virion transport, described by the Boltzmann transport equation. If the virion density is isotropic, the distribution can be approximated as independent of the virion's motion direction. Under this approximation, the Boltzmann transport equation reduces to the

diffusion equation as:

$$\frac{\partial n_v(\vec{r}, t)}{\partial t} = D \nabla^2 n_v(\vec{r}, t) - \Sigma_a v n_v(\vec{r}, t) + S(\vec{r}, t). \quad (9)$$

Where $n_v(\vec{r}, t)dV$ is the number of virions in the volume element dV around the spatial point \vec{r} . $D \nabla^2 n_v(\vec{r}, t)dV$ denotes the virions diffusing into dV per unit time at time t , $\Sigma_a v n_v(\vec{r}, t)dV$ the virions absorbed in dV per unit time at time t . $S(\vec{r}, t)dV$ denotes the virions generated in dV per unit time at time t . D is the diffusion coefficient, v the virion velocity, and Σ_a the macroscopic absorption cross section. In equation (9), it is assumed that all coefficients are position-independent and averaged over the virion velocity distribution. However, the coefficients may be time-dependent as the medium's properties can change over time due to intrinsic factors and external influences. This is known as the single-speed approximation, where all physical processes in the V-reactor are considered to occur at an average velocity, with $n_v(\vec{r}, t)$ accounting for particles with all velocities. Considering the production of progeny virions in the virion replication, the source term can be expressed as:

$$S(\vec{r}, t) = k_\infty \Sigma_a v n_v(\vec{r}, t) + S_0(\vec{r}, t), \quad (10)$$

where the $k_\infty \Sigma_a v n_v(\vec{r}, t)$ is the virion production rate, and k_∞ is the effective multiplication constant for an infinite medium, accounting for virions produced per absorption without leakage loss, and $S_0(\vec{r}, t)$ the virion free source.

Virion kinetic equation. The solution obtained to Eq.(9) is based on the assumption that the variables are separable, specifically that the density is the product of a time-dependent and a spatial-dependent factors:

$$n_v(\vec{r}, t) = f(\vec{r}) n_v(t). \quad (11)$$

By substituting this equality, the diffusion equation Eq.(9) becomes

$$\frac{dn_v(t)}{dt} = D v \frac{\nabla^2 f(\vec{r})}{f(\vec{r})} n_v(t) - \Sigma_a v n_v(t) + k_\infty \Sigma_a v n_v(t) + \frac{S_0(\vec{r}, t)}{f(\vec{r})}. \quad (12)$$

The spatial dependence must satisfy the Helmholtz wave equation,

$$\nabla^2 f(\vec{r}) + B^2 f(\vec{r}) = 0. \quad (13)$$

Where B^2 is the buckling factor, so that the term $\nabla^2 f/f$ is independent of position \vec{r} , and the spatial distributions of S_0 and f are as the same as each other, and then we may set $q(t) \equiv S_0(\vec{r}, t)/f(\vec{r})$. For the infinite assembly the mean virion lifetime, ℓ_∞ , is defined as $\ell_\infty = 1/v\Sigma_a$, and the diffusion length, L , is defined as $L^2 = D/\Sigma_a$. Substituting Eq. (13) into Eq. (12), we get:

$$\frac{dn_v(t)}{dt} = \frac{k_\infty - (1 + L^2 B^2)}{\ell_\infty} n_v(t) + q(t). \quad (14)$$

For a finite assembly, the multiplication constant is k_{eff} , and the virion mean lifetime is ℓ_0 . There is no virion leakage in an infinite assembly, however, finite assemblies, like V-reactor, do experience virion leakage. The relationships for finite and infinite assemblies are:

$$k_{eff} = \frac{k_\infty}{1 + L^2 B^2}, \quad \ell_0 = \frac{\ell_\infty}{1 + L^2 B^2}. \quad (15)$$

Where $1/(1 + L^2 B^2)$ represents the fraction of virions which escape leakage. By substituting Eq. (15), Eq. (14) becomes:

$$\frac{dn_v(t)}{dt} = \frac{k_{eff} - 1}{\ell_0} n_v(t) + q(t). \quad (16)$$

The kinetic parameters for the V-reactor are the reactivity ρ and the virion generation time ℓ , and can be expressed as:

$$\rho = \frac{k_{eff} - 1}{k_{eff}}, \quad \ell = \frac{\ell_0}{k_{eff}}. \quad (17)$$

By substituting Eq.(17), Eq. (16) becomes:

$$\frac{dn_v(t)}{dt} = \frac{\rho}{\ell} n_v(t) + q(t). \quad (18)$$

For the V-reactor without the free source, $q(t) = 0$, we obtain the virion kinetic equation:

$$\frac{dn_v(t)}{dt} = \frac{\rho}{\ell} n_v(t). \quad (19)$$

Eq.(19) describes how the virion density changes over time, and it is applicable throughout a thermal, bare (no reflector) homogeneous reactor, where the virion density is assumed to be uniform in the reactor core. This kinetic equation may be considered as for the point reactor model, commonly known in the nuclear reactor physics.

Solution of virion kinetic equation. The limits of integration for Eq.(19) are $n_v(t) = n_v^0$ at $t = 0$, $\rho = 0$ at $t < 0$, $\rho = \rho$ at $t = 0^+$ and $n_v(t) = n_v(t)$ at $t = t$. Generally, the reactivity is time-dependent, while the generation time may be regarded as a constant, and the solution can be expressed as:

$$n_v(t) = n_v^0 \exp\left(\frac{1}{\ell} \int_0^t \rho(t) dt\right). \quad (20)$$

An analytical solution exists when $\rho(t)$ is integrable. For example, by assuming the reactivity as a linearly decreasing function with time, $\rho(t) = \rho_0 - \gamma t$, we get:

$$n_v(t) = n_v^0 \exp\left(\frac{\rho_0}{\ell} t - \frac{\gamma}{2\ell} t^2\right), \quad (21)$$

where n_v^0 is the initial virion density, $\rho_0 \geq 0$, and $\gamma \geq 0$.

Reactivity and Generation time. The reactivity and the generation time are the two fundamental kinetic parameters in the V-reactor dynamics. By counting the production and destruction of virions, the reactivity is equal to the ratio of net production to production, $\rho = (production - destruction)/production$, and the generation time ℓ is the reciprocals of the production rate, and they can be expressed as:

$$\rho = \frac{v\Sigma_r - (\Sigma_a + DB^2)}{v\Sigma_r}, \quad \ell = \frac{1}{v\Sigma_r}. \quad (22)$$

Where $v\Sigma_r$ represents the virion production rate, v is the average number of virions produced per replication reaction, and Σ_r is the macroscopic cross section for replication reaction. $v\Sigma_a$ and vDB^2 represent the average number of virions lost per unit time due to absorption and leakage, respectively. Σ_a is the macroscopic absorption cross section, representing the probability of absorption events per centimeter of length that the virion traveled.

Cross sections. The reactions between incident and target particles are characterized by the quantity known as the microscopic cross section, which represents the probability of a reaction event of a given type as a function of the kinetic energy of the incident particle. V-reactor dynamics as a quantum-mechanical framework for modeling interactions between "alive particles" (virions and cells) is fascinating. This approach seems to bridge quantum mechanics with virology - a bold and unconventional direction, it

treats virions and cells as quantum-mechanical entities with defined cross sections. Based on quantum mechanics, the cross section for an incident particle (point-sized) striking a target particle is given by $\pi(\lambda_d + R)^2$, where R denotes the radius of the target particle, and λ_d is the de Broglie wavelength of the incident particle, expressed in terms of the particle's kinetic energy, $E = mv^2/2$, as $\lambda_d = h/\sqrt{2Em}$. Where the Planck's constant, $h = 6.626 \times 10^{-27}$ erg sec, m is the mass of the particle in grams, and the velocity v in centimeters per second. By adopting the virion mass of $m_v = 1.0 \times 10^{-15}$ g, and the thermal temperature of $T = 39^\circ\text{C}$, the virion will travel with thermal energy of 0.027 eV, corresponding to $\lambda_d \sim 1.14 \times 10^{-13}$ cm, about ten orders of magnitude smaller than the diameter of the H-particle. This implies that the quantum effects, through the wavelengths, are negligible in an evaluation of thermal virion cross sections. Here, we point out that as an essential difference from the reactions between neutron with nuclide, the cross sections for the absorption or replication reactions of virion with H-particle are not in consistency with the cross-sectional area of H-particle, but become much smaller due to the effects of the biological building components of cell. It has been recognized that the virus enters cells by bidding the spikes (spike glycoprotein) expressed on the surface of virion to the ACE2 (angiotensin-converting enzyme 2) receptors expressed on the surface of cells^[14]. The interface for invasion between virion and H-particle is called receptor-binding domain (RBD) of the SARS-CoV-2 spike protein banding to the ACE2 receptor, attached using a single tail to the outer cell membrane. The RBD of the spike protein is approximately 4.8 - 4.9 nanometers in diameter, as reported in the study^[15]. We introduce the effective cross-sectional area as a measure of the cross section for replication or absorption reaction of virion with H-particle, which is the sum of the RBDs that the H-particle presents to the incoming virion, and approximately estimated as the product of the RBD and the half number of ACE2s of a H-particle. The number of ACE2 per H-particle was found to vary widely, ranging from a few to hundreds, depending on the individuals^[16, 17]. By adopting RBD = 1.85×10^{-13} cm² and considering 300 ACE2 per H-particle, the calculated cross section for the absorption reaction of virion with H-particle is $\sigma_a = 2.775 \times 10^{-11}$ cm², about four orders of magnitude smaller than πR_H^2 . The sizes of the H-particles reported vary significantly, depending on the type of the cells^[18], the radius of the H-particle adopted is $R_H = 3.925 \times 10^{-4}$ cm, and the cross-sectional area is $\pi R_H^2 = 4.84 \times 10^{-7}$ cm². The product of the microscopic cross section σ and the number density of the target particles, N , is termed as the macroscopic cross section, $\Sigma = N\sigma$, representing the probability of reaction events of a given type per centimeter of length that the virion traveled. We note that the absorption cross section σ_a is over estimated by the above way, and it gives actually the cross section for a virus to bind to a cell target, but not to enter into. The recent studies show that binding to the ACE2 receptor is just a critical initial step for SARS-CoV to enter into target cells^[14]. The researches have emphasized the role of ACE2 in mediating entry of SARS-CoV-2^[19, 20], and such mediating effects on the cell entry remain to quantify. Note that $\sigma_a = \sigma_r + \sigma_c$, where σ_c is the cross section for virion capture, meaning that an entering virion was absorbed but without release of progenies. As an approximation, we may neglect σ_c , and thus $\sigma_r = \sigma_a$. The present theory predicts that the σ_r (as replication efficiency) varies widely depending on the type of cells, and cells with higher ACE2 expression can yield folds more virions than low-ACE2 cells.

Burnup equation. The fuel burnup is defined as the change in the concentration of H-particles, which are the targets for the replication reaction induced by virion and regraded as fuel. For a given

thermal virion flux or density, the fuel burnup is determined by the cross sections for the replication and capture reactions. To form the burnup equation, we assume that the H-particle undergoing reapplication or capture reactions will transform to a destroyed H-particle, which is no longer considered as fuel, and the influence of the consumption of H-particles in return on the virion flux is ignorable. The fuel burnup equation can be written as:

$$\frac{dN_H}{dt} = -\phi \sigma_c N_H - \phi \sigma_r N_H. \quad (23)$$

Where N_H represents the number density of the H-particles, ϕ denotes the flux of the thermal monoenergetic virions, and σ_c and σ_r are the capture and replication cross sections, respectively. By using the equality $\sigma_a = \sigma_c + \sigma_r$, Eq. (23) is reduced to:

$$\frac{dN_H}{dt} = -\sigma_a \phi N_H. \quad (24)$$

The solution to Eq. (24) can be expressed as:

$$N_H(t) = N_H^0 \exp(-\sigma_a v_{th} \int_0^t n_v(t) dt). \quad (25)$$

Where the N_H^0 is the initial number density of H-particles, v_{th} the thermal velocity of virions.

Virus transmission. The dynamics of the spreading of the COVID-19 virus has similar features to turbulent flow, chaotic maps, and other non-linear systems: a small perturbation grows exponentially and eventually saturates to a final value. The dynamical control parameter of chaotic systems is termed the Lyapunov Exponent (LE), which quantifies the divergence between two initially infinitesimally close trajectories in phase space over time t , indicating the presence and degree of chaos. To be more specific, we define the relative distance between the two trajectories as a function of time, $d(t) = d_0 \exp(\lambda t)$. For a chaotic system, the specific quantity $d(t)$ can be expressed as^[21, 22]: $d(t) = (d_0 d_\infty) / (d_0 + d_\infty \exp(-\lambda t))$. This equation describes that a small perturbation, indicated by $d_0 = d(t = 0)$, grows exponentially with a coefficient λ , the (LE), and finally saturates to a value $d_\infty = d(t \rightarrow \infty)$. The kinetic equation (19) indicates that the viral load, $n_v(t)$, grows exponentially at a rate characterized by the initial reactivity, ρ_0/ℓ . As the peak viral load dominates the total viral production, its exponential growth, $n_v(t) = n_0 \exp((\rho_0/\ell)t)$, can be interpreted as the chaotic divergence $d(t)$. Within the framework of chaos theory, this defines a chaotic system referred to as viral production chaos, and we can express it as $n_v(t) = (n_0 n_\infty) / (n_0 + n_\infty \exp(-\lambda_v t))$. Where $n_0 = n_v(t = 0)$, $n_\infty = n_v(t \rightarrow \infty)$, and $\lambda_v = \rho_0/\ell$ is the (LE) governing the chaotic growth. To characterize the spread of the virus, we introduce the number of people testing positive for the virus, denoted as $N_{pos}(t)$. We assume a power-law relationship between the fast-varying viral load and the slower-varying case count, $N_{pos}(t) = n_v(t)^\chi = N_0 \exp(\chi(\rho/\ell)t)$, where χ is a dimensionless scaling exponent. This relationship implies that the growth rate of the population-level outbreak is scaled by the exponent χ . Consequently, the (LE) for the population transmission chaos is given by the scaling law: $\lambda = \chi \lambda_v$. The value of the scaling exponent χ , which couples the intra-host and population-level dynamics, can be determined experimentally. By interpreting $N_{pos}(t)$ as the chaotic divergence $d(t)$, we obtain the equation for population-level transmission:

$$N_{pos}(t) = \frac{N_0 N_\infty}{N_0 + N_\infty \exp(-\lambda t)}, \quad (26)$$

where d (in days) represents the time from the starting of the epidemic or the beginning of testing to isolate the virus, $N_0 =$

$N_{pos}(t = 0)$ is the initial number of people infected, and $N_{\infty} = N_{pos}(t \rightarrow \infty)$ denotes the final number of people infected, characterized by a saturation value.

References

- [1] Zhou, P et al. A pneumonia outbreak associated with a new coronavirus of probable bat origin, *Nature* 579, 270-273 (2020).
- [2] Coronavirus data 2020 at: <https://coronavirus.jhu.edu/>
- [3] Cheng VC, Lau SK, Woo PC, Yuen KY. Severe acute respiratory syndrome Coronavirus as an agent of emerging and reemerging infection. *Clin Microbiol Rev* 20, 660-94 (2007).
- [4] World Health Organization. (2024, May 7). Draft outcome of the WHO Pandemic Agreement (Document A/INB/7/3). https://apps.who.int/gb/inb/pdf_files/inb7/A_INB7_3_en.pdf
- [5] Chu Hin. et al. Comparative Replication and Immune Activation Profiles of SARS-CoV-2 and SARS-CoV in Human Lungs: An Ex Vivo Study With Implications for the Pathogenesis of COVID-19. *CID* 71, 1400-1409 (2020).
- [6] R. Wolfel, VM. Corman, W. Guggemos, et al., Virological assessment of hospitalized patients with COVID-2019 *Nature* 581, 465-469 (2020) <http://dx.doi.org/10.1038/s41586-020-2196-x>.
- [7] Y. Pan, D. Zhang, P. Yang, L.L.M. Poon, Q. Wang, Viral load of SARS-CoV-2 in clinical samples, *Lancet Infect. Dis.* (2020) S1473-3099(20)30113-4. [http://dx.doi.org/10.1016/S1473-3099\(20\)30113-4](http://dx.doi.org/10.1016/S1473-3099(20)30113-4). PubMed PMID: 32105638.
- [8] Sunpeng Wang, Yang Pan, Quanyi Wang, Hongyu Miao, Ashley N. Brown, Libin Rong, Modeling the viral dynamics of SARS-CoV-2 infection *Mathematical Biosciences* 328 (2020) 108438 <https://doi.org/10.1016/j.mbs.2020.108438>
- [9] Peiris JS, Chu CM, Cheng VC, et al., Clinical progression and viral load in a community outbreak of coronavirus associated SARS pneumonia: a prospective study *Lancet* 361: 1767-1772 (2003).
- [10] Ron Sender, Yinon M. Bar-On, Shmuel Gleizer, et al., The total number and mass of SARS-CoV-2 virions *PNAS* Vol. textbf(118) No. 25 e2024815118 (2021) <https://doi.org/10.1073/pnas.2024815118>
- [11] Michael A. Johansson, Talia M. Quandelacy, Sarah Kada, et al. SARS-CoV-2 Transmission From People Without COVID-19 Symptoms *JAMA Network Open*. 2021;4(1):e2035057. doi:10.1001/jamanetworkopen.2020.35057
- [12] Eskild Petersen, Marion Koopmans, Unyeong Go, et al. Comparing SARS-CoV-2 with SARS-CoV and influenza pandemics www.thelancet.com/infection Vol 20 August 2020, e238 - e244.
- [13] Hongkong and Shanghai coronavirus data 2022: https://wp.m.163.com/163/page/news/virus_report/index.html?_nw=1&_anw=1, https://news.sina.cn/zt_d/yiqing0121
- [14] Jun Lan, Jiwan Ge, Jinfang Yu, et al. Structure of the SARS-CoV-2 spike receptor-binding domain bound to the ACE2 receptor *Nature* 581, 215-220 (2020) doi.org/10.1038/s41586-020-2180-5
- [15] Cecylia S. Lupala, Yongjin Ye, Hong Chen, Xiao-Dong Su, Haiguang Liu. Mutations on RBD of SARS-CoV-2 Omicron variant result in stronger binding to human ACE2 receptor *Biochemical and Biophysical Research Communications* 590, 34e41 (2022). <https://doi.org/10.1016/j.bbrc.2021.12.079>
- [16] Hao Xu, Liang Zhong, Jiaxin Deng, et al. High expression of ACE2 receptor of 2019-nCoV on the epithelial cells of oral mucosa *International Journal of Oral Science* (2020) 12:8 <https://doi.org/10.1038/s41368-020-0074-x>
- [17] Guoping Li, Xiang He, Lei Zhanga, et al. Assessing ACE2 expression patterns in lung tissues in the pathogenesis of COVID-19 *Journal of Autoimmunity* 112 (2020) 102463 <https://doi.org/10.1016/j.jaut.2020.102463>
- [18] James D. Craop, Brenda E. Barry, Peter Gehr, et al., Cell Number and Cell Characteristics of the Normal Human Lung DOI: 10.1164/arrd.1982.126.2.332
- [19] Walls, A. C. et al. Structure, function, and antigenicity of the SARS-CoV-2 spike glycoprotein. *Cell* <https://doi.org/10.1016/j.cell.2020.02.058> (2020).
- [20] Hoffmann, M. et al. SARS-CoV-2 cell entry depends on ACE2 and TMPRSS2 and is blocked by a clinically proven protease inhibitor. *Cell* <https://doi.org/10.1016/j.cell.2020.02.052> (2020).
- [21] Ott E. Chaos in dynamical systems, Cambridge University Prtess, Englandf, 1993; Hilborn RC. Chaos an nonlinear dynamics, Oxford University Prtess, New York, 1994.
- [22] Bonasera A, Latora V and Rapisarda A. *Phys. Rev. Lett.* (1995) 75, 3434.